Effective temperatures and the breakdown of the Stokes-Einstein relation for particle suspensions

Carlos I. Mendoza, I. Santamaría-Holek, and A. Pérez-Madrid

Articles you may be interested in

Breakdown of the Stokes-Einstein relation in two, three, and four dimensions
J. Chem. Phys. **138**, 12A548 (2013); 10.1063/1.4792356

Nature of the breakdown in the Stokes-Einstein relationship in a hard sphere fluid
J. Chem. Phys. **124**, 214501 (2006); 10.1063/1.2192769

Hydrodynamic boundary conditions, the Stokes–Einstein law, and long-time tails in the Brownian limit
J. Chem. Phys. **119**, 8062 (2003); 10.1063/1.1610442

Viscoelasticity and generalized Stokes–Einstein relations of colloidal dispersions
J. Chem. Phys. **111**, 8721 (1999); 10.1063/1.480212

Breakdown of the Stokes–Einstein relation in supercooled liquids
J. Chem. Phys. **103**, 3071 (1995); 10.1063/1.470495

Effective temperatures and the breakdown of the Stokes-Einstein relation for particle suspensions

Carlos I. Mendoza,[1] I. Santamaría-Holek,[2] and A. Pérez-Madrid[3]

[1]*Instituto de Investigaciones en Materiales, Universidad Nacional Autónoma de México, Apdo. Postal 70-360, 04510 México, D.F., Mexico*
[2]*UMDI-Facultad de Ciencias, Universidad Nacional Autónoma de México Campus Juriquilla, 76230 Querétaro, Mexico*
[3]*Departament de Física Fonamental, Universitat de Barcelona, Marti i Franques 1, 08028 Barcelona, Spain*

The short- and long-time breakdown of the classical Stokes-Einstein relation for colloidal suspensions at arbitrary volume fractions is explained here by examining the role that confinement and attractive interactions play in the intra- and inter-cage dynamics executed by the colloidal particles. We show that the measured short-time diffusion coefficient is larger than the one predicted by the classical Stokes-Einstein relation due to a non-equilibrated energy transfer between kinetic and configuration degrees of freedom. This transfer can be incorporated in an effective kinetic temperature that is higher than the temperature of the heat bath. We propose a Generalized Stokes-Einstein relation (GSER) in which the effective temperature replaces the temperature of the heat bath. This relation then allows to obtain the diffusion coefficient once the viscosity and the effective temperature are known. On the other hand, the temporary cluster formation induced by confinement and attractive interactions of hydrodynamic nature makes the long-time diffusion coefficient to be smaller than the corresponding one obtained from the classical Stokes-Einstein relation. Then, the use of the GSER allows to obtain an effective temperature that is smaller than the temperature of the heat bath. Additionally, we provide a simple expression based on a differential effective medium theory that allows to calculate the diffusion coefficient at short and long times. Comparison of our results with experiments and simulations for suspensions of hard and porous spheres shows an excellent agreement in all cases. © *2015 AIP Publishing LLC.* [http://dx.doi.org/10.1063/1.4930550]

I. INTRODUCTION

The Stokes-Einstein relation (SER) is one of the fundamental results of the theory of Brownian motion that establishes the correlations between the uptake and dissipation of energy by a system of particles that are in contact with a heat bath. The practical importance of the SER is that it establishes a simple quantitative relation between the diffusion coefficient of the particles, D_0, and the viscosity of the heat bath, η_0, through

$$D_0 \eta_0 = \frac{k_B T_0}{6\pi a}, \qquad (1)$$

where k_B is the Boltzmann's constant, T_0 is the heat bath temperature, and a is the radius of the suspended particles. Although Eq. (1) has been deduced in the infinite dilute case, it can be generalized to finite volume fractions ϕ in the form

$$D(\phi)\eta(\phi) = \frac{k_B T_0}{6\pi a}, \qquad (2)$$

where $D(\phi)$ and $\eta(\phi)$ are the relative concentration dependent diffusion and viscosity coefficients.

For many years, this relationship has been experimentally and numerically tested in many systems ranging from diluted to highly concentrated colloidal suspensions and glasses.[1–6] A parametric representation of the SER obtained for colloidal suspensions is shown in Fig. 1 where we plot the inverse of the effective viscosity (at infinite and zero frequencies) versus the diffusion coefficient (at short and long times, respectively)

of the suspension. The SER, Eq. (2), is represented by the gray dotted straight line. Experimental and simulation results (symbols) clearly indicate a breakdown at short and long times even at low volume fractions. This breakdown of the SER is very general since other systems show similar features, for example, quenched fragile molecular systems experiencing glass transition.[7,8]

Many attempts to understand this breakdown can be found in the literature, see, among many others, Refs. 9–13. For particle suspensions, the problem has been usually approached from the point of view of hydrodynamic interactions and mode coupling (MC) that lead to descriptions incorporating memory and non-Markovian effects. These micro-mechanical points of view imply complicated mathematical manipulations involving infinite hierarchies of evolution equations that should be approximated in order to obtain useful formulas. On the other hand, simple non-Markovian models have also been proposed that give approximate expressions for the generalized Stokes-Einstein relation (GSER). However, they are unable to cope with the dependence of viscosity and diffusion on the volume fraction.

Our aim in this work is to present a novel approach to the problem in which physical mechanisms associated with energy transfer between different degrees of freedom are considered. Formally, we base our considerations on the idea that a solution of particles can be described as an effective medium whose transport properties depend on the volume fraction. Thus, our
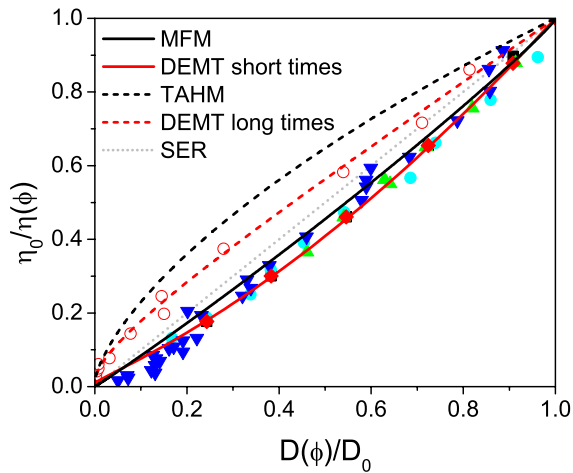
FIG. 1. Breakdown of the Stokes-Einstein relation (SER) for short (solid lines) and long times (dashed lines). Symbols represent data from experiments and simulations taken from Refs. 3–5 and 12–17. In all the lines, the vertical axis corresponds to the viscosity given by the differential effective medium theory (DEMT) given by Eq. (11) with $c = 0.22$ for short times and $c = 0.57$ for long times. The grey dotted straight line representing the Stokes-Einstein relation (SER) is obtained after using Eq. (2) to obtain the diffusion coefficient. The black solid line is the short-time mean field model (MFM) for the diffusion coefficient obtained using Eqs. (3), (10), and (11). The red solid line is the short-time DEMT given by Eq. (19) with $c_D = 0.38$ and $\lambda = -1.83$. The black dashed line corresponds to the long-time thermally activated hopping model (TAHM) for the diffusion given by Eq. (18). The red dashed line is the long-time DEMT using the crowding parameter $c_D = 0.75$ and $\lambda = -2.89$ for the diffusion given by Eq. (19).

explanation and quantitative description of the breakdown of the SER are based on a thermodynamic-like approach that we correlate with the mesoscopic dynamics of the particles at short and long times by using Fokker-Planck and diffusion equations, respectively.

We show how the intra- and inter-cage dynamic mechanisms[18] are at the origin of the differences between the short- and long-time diffusion of tracer particles, and we deduce simple and accurate quantitative expressions for the volume-fraction dependent diffusion coefficients $D(\phi)$ at short and long times. The deduction of these diffusion coefficients together with previous results on the dependence of the viscosity on the volume fraction[19] and the independent calculation of an effective temperature (at short times) allow us to justify and validate a formula accounting for the generalized Stokes-Einstein relation.

In general terms, the picture of the process is as follows. At short times, the diffusion coefficient of tracer particles during their intra-cage diffusion is larger than that predicted by the SER, Eq. (1), as evidenced by the solid lines in Fig. 1. This is a consequence of the existence of strong confining forces, originated by the presence of the other suspended particles that delay the relaxation of the velocities to their equilibrium distribution. This lack of equilibration provides an extra energy supply for tracer particle fluctuations, that is, an increased thermal energy that may be quantified in terms of an "effective temperature" larger than that of the host fluid.[20] A simple formula accounting for this deviation will be derived here on the basis of the Fokker-Planck equation for the distribution function of the tracer particles.

The long-time behavior in turn is characterized by a diffusion coefficient smaller than that predicted by the SER (see dashed lines in Fig. 1). In this case, the inter-cage dynamics slows down diffusion due to a sequence of thermally activated hopping processes and attractive interactions of hydrodynamic origin. A theoretical formula accounting for this behavior will be deduced following an approach similar to that originally proposed by Eyring that takes into account important features of the dynamics of colloidal particles.[21,22] Finally, we use an accurate differential effective medium formalism to obtain simple analytical expressions giving a close quantitative fit of experimental data for the short- and long-time diffusion coefficient in the complete range of volume fractions.[19] Here, we propose that the viscosity and the diffusion coefficient can be related by means of a GSER of the form

$$\frac{D(\phi)}{D_0}\frac{\eta(\phi)}{\eta_0} = \frac{T(\phi)}{T_0}, \tag{3}$$

where the effective temperature $T(\phi)$ replaces the temperature of the bath. This relation can be used at short and long times to express one of the three quantities it contains in terms of the others.

The article is organized as follows. In Section II, we present the analysis of the short-time dynamics of the system by briefly reviewing a mean field model (MFM) based on a reduction of the Fokker-Planck equation for the velocity and position dependent distribution function. After this, we propose a confinement potential that allows us to obtain an explicit expression for the effective temperature. In Section III, we analyze the long-time behavior by introducing a thermally activated hopping model (TAHM) that allows to calculate in a very simple way, the long-time diffusion coefficient of the colloidal particles. In Section IV, we obtain an expression for the diffusion coefficient valid at short and long times by using a differential effective medium approach that we briefly outline. Finally, in Section V, we discuss our results and present our conclusions.

II. SHORT TIMES: MFM

The solid symbols in Fig. 2 show the experimental and simulation data for the short-time diffusion coefficient $D_{st}(\phi)$. The dotted line is the result of the volume fraction dependent Stokes-Einstein relation, Eq. (2). Although the quantitative agreement between the experimental data and Eq. (2) is satisfactory until volume fractions about $\phi = 0.2$, then Eq. (2) slightly under-estimates the diffusion coefficient at higher volume fractions. This difference can be explained by analyzing carefully the effect of confining forces on the relaxation of the velocity of the suspended particles. This task can be accomplished by using a Fokker-Planck equation for the phase space probability density $f(\mathbf{r}, \mathbf{v}, t)$ of a tracer particle, where $\mathbf{r}$ and $\mathbf{v}$ are its position and velocity, respectively,

$$\frac{\partial f}{\partial t} + \frac{\partial}{\partial \mathbf{r}} \cdot (\mathbf{v}f) = \epsilon \frac{\partial}{\partial \mathbf{v}} \cdot \left[\frac{\partial}{\partial \mathbf{r}} U(\mathbf{r}; \phi)f \right]$$
$$+ \gamma \frac{\partial}{\partial \mathbf{v}} \cdot \left[\mathbf{v}f + \frac{k_B T_0}{m} \frac{\partial f}{\partial \mathbf{v}} \right]. \tag{4}$$
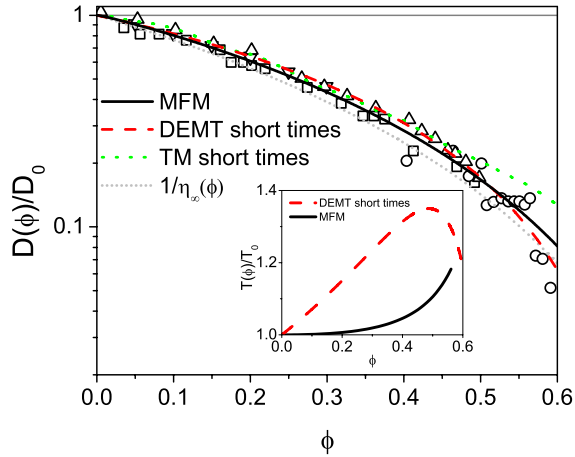
FIG. 2. Short-time effective diffusion coefficient as a function of the volume fraction. The gray dotted line corresponds to the inverse of the infinite frequency viscosity given by Eq. (11) with $c = 0.22$. The black solid line is the mean field model (MFM) prediction given by Eqs. (3), (10), and (11). The dashed red line is the prediction of the differential effective medium theory (DEMT) with $c_D = 0.38$ and $\lambda = -1.83$ in Eq. (19). Finally, the green dotted line is the prediction given by the Tokuyama model (TM) of Ref. 12. The inset shows the effective temperature predicted by the indicated models. Data taken from Ref. 5.

Here, γ is the constant friction coefficient per unit of mass that the tracer particle experiences as it moves through the host fluid ($\gamma = 6\pi a\eta_0$). $U(\mathbf{r}; \phi)$ represents an effective potential energy per unit of mass arising from the interaction of the tracer particle with the neighboring colloidal particles which form cages that restrict the movement of the tracer. The force associated with this potential energy therefore arises from the *effective* heat bath, made up of the host fluid and the other colloidal particles, and it is mediated by the coupling coefficient ϵ and depends on the particle volume fraction $\phi = Nb/V$, with N the number of particles in suspension, $b = 4\pi a^3/3$ the volume of each particle, and V the total volume of the system. The coupling parameter $\epsilon = (ma^2/6k_BT)\gamma^2$ is an Onsager coefficient that brings in the effects on the interactions coming from the finite-size of the particles. The relation for ϵ has been obtained with the help of the generalized Faxén theorem in Ref. 23.

The expression for the volume-fraction dependent effective temperature can now be obtained from Eq. (4). The existence of the strong confining forces prevents the relaxation of the velocities of the particles to their equilibrium distribution before a diffusive change of configuration of the system is appreciable. As a consequence, there exists a coupling between the two degrees of freedom, $\mathbf{r}$ and $\mathbf{v}$, and the probability density $f(\mathbf{r}, \mathbf{v}, t)$ cannot be factorized as a product of two independent functions, as it is usually done when deriving the Smoluchowski equation from the Fokker-Planck equation.[20] Instead, we have to consider that $f = h_{\mathbf{r}}(\mathbf{v}, t)\rho(\mathbf{r}, t)$ with $h_{\mathbf{r}}(\mathbf{v}, t)$ standing for the conditional probability of the velocity for a given spatial configuration of the particles. The Smoluchowski equation describing the diffusion regime can then be deduced by using this expression for the probability density and contracting the description over velocities.[20] In a mean field approximation, the resulting equation for $\rho(\mathbf{r}, t)$ contains a diffusion term with increased thermal energy which

is proportional to the mean-field effective temperature[20]

$$\frac{T(\phi)}{T_0} = 1 + \frac{1}{3}\gamma^{-2}\langle[\nabla U(\mathbf{r}; \phi)]^2\rangle. \quad (5)$$

The fact that $T(\phi) > T_0$ means that the tracer particle has an extra energy disposal to perform fluctuations due to the fact that the velocities have not yet relaxed to their equilibrium distribution. An explicit expression for $T(\phi)$ can be deduced if we model the confinement forces by means of an harmonic force with a spring constant that depends on particle concentration, $k(\phi)$. The corresponding relation for the potential energy is[20]

$$U(\mathbf{r}; \phi) = U_0 + \frac{1}{2}\omega^2(\phi)\sum_{i=1}^{3} r_i^2, \quad (6)$$

where r_i are the cartesian components of the position vector and $\omega(\phi) = \sqrt{k(\phi)/m}$ is the corresponding characteristic frequency associated to the spring constant of the harmonic potential. Substituting now Eq. (6) into (5) we derive the general expression

$$\frac{T(\phi)}{T_0} = 1 + \gamma^{-2}\frac{m}{3\,k_BT_0}\epsilon^2\omega^4(\phi)\langle r^2(t)\rangle, \quad (7)$$

where $\langle r^2(t)\rangle$ is the mean square displacement of the tracer particles.

Confining forces can be attributed to the formation of cages within the suspension. The tracer particles move inside the cages at short times and jump between cages at long times. The characteristic size Λ of these cages can be written as $\Lambda \simeq V_{free}^{1/3}$, where the available volume a tracer particle can occupy is $V_{free} = V(1 - \phi_{eff})$ with the effective volume fraction given by $\phi_{eff} = \phi(1 - c\phi)^{-1}$ and the packing constant $c = (1 - \phi_c)/\phi_c$, with ϕ_c the critical volume fraction when dynamic arrest occurs.[19] Taking into account that the free volume can also be written in the form $V_{free} = h(V^{1/3} - 2a)^3$, with h a free parameter that depends on the packing of the particles,[22] then

$$\Lambda(\phi) = 2ah\frac{(1 - \phi_{eff})^{1/3}}{h - (1 - \phi_{eff})^{1/3}}. \quad (8)$$

Comparing now the mean kinetic energy of the particles, $E_c = 3k_BT_0/2m$, with the maximum potential energy available, $U^{max} = \frac{1}{2}\omega^2(\phi)\Lambda^2(\phi)$, we obtain the simple relation

$$\omega^2(\phi) = \frac{3k_BT_0}{m\Lambda^2}. \quad (9)$$

For a harmonically bounded particle $\langle r^2(t)\rangle = k_BT(\phi)/[m\epsilon\omega^2(\phi)]$ and therefore, after using Eq. (9), the effective mean-field temperature takes the simple form

$$\frac{T(\phi)}{T_0} = \frac{\Lambda_{h=1}^2(\phi)}{\Lambda_{h=1}^2(\phi) - a^2}, \quad (10)$$

where we have assumed that for short-times $h = 1$ because at short times and low concentrations, the cage radius should diverge.

Once the effective temperature has been obtained, one can use the GSER, Eq. (3), to obtain the diffusion coefficient. For this purpose, we need an expression for the viscosity as function of the volume fraction. Here, we use the effective

viscosity[19]

$$\eta(\phi) = \eta_0 \left(1 - \frac{\phi}{1 - c\phi}\right)^{-[\eta]}, \tag{11}$$

where $[\eta]$ is the intrinsic viscosity and $c = 0.22$, for the infinite frequency case. It has been shown in Ref. 19 that this expression for the viscosity accounts very accurately for the dependence of the viscosity on the volume fraction. This expression incorporates, in an effective way, both excluded volume and hydrodynamic interactions.

Due to its effective medium character, it is difficult to obtain insight into particle correlations of hydrodynamic origin based exclusively on this expression. Other methods are more appropriate to achieve such objective, for example, methods based on explicit hydrodynamic analysis.[24–27] However, these micromechanical approaches usually lead to virial representations of the viscosity that have strong quantitative limitations in accounting for the experimental data in the whole volume fraction range. This is due because in practice, only the second virial coefficient can be explicitly obtained. On the other hand, Eq. (11) can be expanded in a virial series from where all the orders of the series can be calculated. A comparison of the virial expansion of Eq. (11) gives values for the second virial coefficients that are very similar to the ones reported by the mentioned hydrodynamic calculations.

After substituting Eqs. (10) and (11) into (3), we obtain the short-time diffusion coefficient shown by the black solid line in Figs. 1 and 2. A good agreement between theory, experiments, and simulations is obtained.

Summarizing, in this section, we have calculated an effective temperature based on the assumption that the velocities of the particles do not relax to their equilibrium distribution. This result, together with the GSER and the knowledge of the dependence of the viscosity on the volume fraction, allowed us to obtain a diffusion coefficient that reproduces very good experimental data. This fact is *a posteriori* justification of the initial hypothesis that the viscosity and the diffusion coefficient are related by Eq. (3). It is worth emphasizing that, if $T(\phi)$ is replaced by T_0 in Eq. (3), one recovers the volume fraction dependent Stokes-Einstein relation, Eq. (2). Thus, its breakdown is due to the fact that the effective temperature is different from the temperature of the bath. But we have shown that at short times, this difference is due to the fact that velocities have not relaxed to their equilibrium value, otherwise $T(\phi)$ would reduce to T_0. This also means that the breakdown occurs even at small volume fractions, long before freezing starts, as shown in Fig. 1.

III. LONG TIMES: TAHM

The previous results explain how the effect of confining forces affect the dynamics of the tracer particle inside a cage formed by other particles at short times. However, at long times, the effect of confining forces on the inter-cage dynamics of the tracer particle is governed by diffusion through a periodic potential, and therefore, it may be considered as a sequence of thermally activated hopping processes that can be analyzed in terms of the theory of rate processes.[21,22] The long-

time behavior of the diffusion coefficient can be explained by considering that the equation governing the diffusion of the tracer particle in the effective medium is of the form

$$\frac{\partial \rho}{\partial t} = \nabla \cdot [D_l(\phi) \nabla \rho], \tag{12}$$

with ρ the single particle distribution function. According to the theory of rate processes,[22] the effective long-time diffusion coefficient $D_l(\phi)$ is given by

$$D_l = D_0 \frac{\Lambda^2(\phi)}{4a^2 h^2} \left(1 + \phi \frac{\partial \ln|\gamma(\phi)|}{\partial \phi}\right), \tag{13}$$

where $\gamma(\phi)$ is the activity coefficient and $\Lambda(\phi)$ is the characteristic length. For particle suspensions, this quantity strongly depends on the volume fraction, as it is shown in Eq. (8).

If we assume that the suspension behaves as a hard sphere gas and that Λ is a constant, one obtains for the long-time diffusion coefficient $D_l^{hs} \sim (1 - c\phi)^{-2}$, which diverges at $\phi = 1.57$. This unexpected behavior is due to the fact that the activity coefficient for hard spheres is a monotonically increasing function of the volume fraction.

The previous results suggest that, in order to reproduce the experimental data when the diffusion goes to zero, some type of effective attractive interactions (possibly coming from hydrodynamic interactions or capilar forces) should be taken into account. Assuming for simplicity that the suspended particles follow a van der Waals-like description, where the pressure is given by

$$P(\phi) = \frac{k_B T_0}{b} \frac{\phi}{1 - c\phi} - \frac{\alpha}{b^2} \phi^2, \tag{14}$$

with b the volume of a particle, α a coefficient associated with attractive interactions, and where we have included the crowding factor c. In order to obtain the activity coefficient, we use the following relation for the fugacity $f(\phi)$:[28]

$$\log\left[\frac{f}{\rho}\right] = \int (Z - 1) \frac{d\rho}{\rho}, \tag{15}$$

where we introduced the compressibility factor $Z = \frac{b}{k_B T} \frac{P(\phi)}{\phi}$. After performing the integrals, we can deduce the expression of the chemical potential $\mu(\phi)$,

$$\mu(\phi) = k_B T_0 \log\left[\frac{\phi}{1 - c\phi} e^{R(\phi)}\right]. \tag{16}$$

From this equation, we may identify the activity coefficient,

$$\gamma_{vdw}(\phi) = \frac{1}{1 - c\phi} e^{R(\phi)}, \tag{17}$$

where $R(\phi) = -2A\phi + 1/(1 - c\phi)$, with $A = \alpha/bk_B T_0$ a parameter measuring the intensity of the attractive interactions. Substituting Eq. (17) into Eq. (13), one obtains the long-time diffusion coefficient,

$$\frac{D_l^{TAHM}}{D_0} = \frac{(1 - \phi_{eff})^{2/3}}{[2 - (1 - \phi_{eff})^{1/3}]^2} \left(\frac{1}{(1 - c\phi)^2} - A\phi\right). \tag{18}$$

Equation (18) constitutes the TAHM model represented by the solid black line in Fig. 3, in which we compare with experimental data and other models shown in the caption. The fit was done using $h = 2$ because for long times and high volume
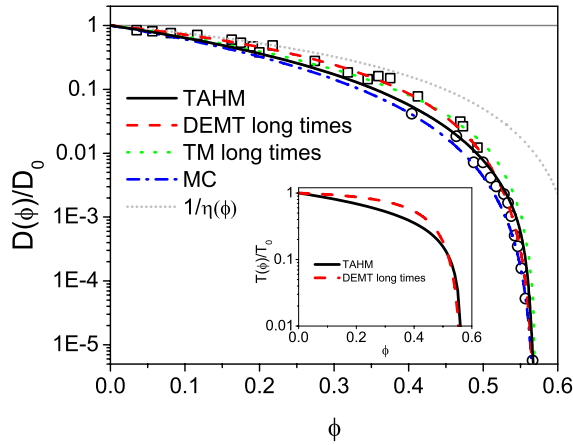
FIG. 3. Long-time effective diffusion coefficient as a function of the volume fraction. The gray dotted line corresponds to the inverse of the viscosity given by Eq. (11) with $c = 0.57$. The solid black line is the prediction of the thermally activated hopping model (TAHM), Eq. (18) with $A = 3.851$. The dashed red line corresponds to the differential effective medium theory (DEMT) prediction, Eq. (19), using the values $c_D = 0.75$ and $\lambda = -2.89$. The blue dashed-dotted line is the mode coupling (MC) prediction of Ref. 13 whereas the green dotted line corresponds to the Tokuyama model (TM) deduced in Ref. 12 The inset shows the effective temperature predicted by the indicated models. Data taken from Ref. 5.
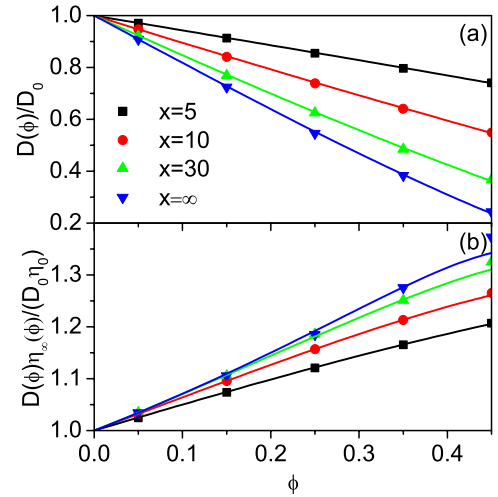

FIG. 4. (a) Short-time effective diffusion coefficient as a function of the volume fraction for particles with different porosities. The data (symbols) were taken from the simulations of Refs. 2 and 3. The lines correspond to the differential effective medium theory (DEMT) fittings given by Eq. (19). (b) The generalized Stokes-Einstein relation (GSER), Eq. (3), as a function of the volume fraction. The lines correspond to the DEMT fittings given by Eqs. (11) and (19). The fitting constants are given in Table I. The data (symbols) were taken from the simulations of Ref. 2.

fractions the characteristic length of the cages should be about $2a$. An expression for the long-time diffusion coefficient (green dotted line of Fig. 3) on the volume fraction has been obtained in Ref. 12 by means of a micro-mechanical description based on non-Markovian Langevin equations and a self-consistent expansion method in terms of the volume fraction. The performance of both expressions is remarkable although the method used here to deduce Eq. (18) is much simpler. The results of the MC theory are also shown by the blue dashed-dotted line of Fig. 3.

Using Eqs. (3), (11), (13), and (17), it is possible to determine the corresponding long-time effective temperature of the system. The results are shown in the inset of Fig. 3 for TAHM (solid black line) and the differential effective medium theory (DEMT) (dashed red line) that will be discussed in Sec. IV. The breakdown of the SER arising from the use of the present model are shown in Fig. 1.

IV. SHORT AND LONG TIMES: THE DEMT

A simple expression for the diffusion coefficient, valid at short and long times can be obtained by using a differential effective medium approach. In this procedure, the low volume fraction limit of the diffusion coefficient $D(\phi) = D_0(1 + \lambda\phi)$ is modified to incorporate excluded volume interactions by replacing ϕ in the previous expression with $\phi_{eff} = \phi/(1 - c_D\phi)$. Here, $c_D = (1 - \phi_D)/\phi_D$ is a constant related to the critical volume fraction ϕ_D where the diffusion coefficient vanishes. The first order virial coefficient λ can be determined by using a hydrodynamic approach.[2] Further corrections due to hydrodynamic interactions between particles, which become increasingly important when increasing the volume fraction, are taken into account by a technique based on a progressive addition of particles to the sample, so that the new particles interact in

an effective way with those added in previous stages.[19] Hence, after using the differential effective medium method described in Ref. 19, one obtains the following expression for $D^{DEMT}(\phi)$:

$$D^{DEMT}(\phi) = D_0\left(1 - \frac{\phi}{1 - c_D\phi}\right)^{-\lambda}. \qquad (19)$$

Equation (19) was used to describe experimental data of the short- and long-time diffusion coefficients, as shown by the red dashed lines in Figs. 2 and 3. It is clear that the DEMT fits extremely well the experimental data at all volume fractions.

In addition, combining Eqs. (11) and (19) in the GSER, Eq. (3), we may also deduce the following general expression for the effective temperature corresponding to the DEMT

$$\frac{T_{DEMT}(\phi)}{T_0} = \left(1 - \frac{\phi}{1 - c_D\phi}\right)^{-\lambda_i}\left(1 - \frac{\phi}{1 - c\phi}\right)^{-[\eta]}. \qquad (20)$$

Figure 1 (red lines) shows that the DEMT reproduces correctly all the experimental data that show the breakdown of the SER. We probed the generality of the DEMT by also considering the case of suspensions of homogeneous porous particles and compared its predictions with accurate numerical results

TABLE I. Parameters for the DEMT valid at short times. The values of the crowding factors c_D are obtained from a best fit of Eq. (19) to the numerical simulations of Refs. 1 and 2 for four different porosities x. The first-order virial coefficients λ for the diffusion coefficient are obtained in Ref. 2 We also include the intrinsic viscosity $[\eta]$ and the crowding factor c of the high-frequency viscosity, as given by Eq. (11), obtained in Ref. 29.

x	5	10	30	∞
λ	−0.569	−1.060	−1.550	−1.832
c_D	−0.206	−0.082	0.143	0.384
$[\eta]$	1.076	1.701	2.236	2.500
c	−0.516	−0.355	−0.063	0.223

recently obtained for such systems.[1,3] The comparison of theory (lines) with simulations (symbols) is shown in Fig. 4, after fitting the simulation data of Refs. 1–3 (see the Table I and also Ref. 29).

V. DISCUSSION AND CONCLUSIONS

In this article, we proposed and tested a generalized Stokes-Einstein relation, Eq. (3), valid for colloidal suspensions at arbitrary volume fractions and at short and long times. Our main results are summarized in Eqs. (6)–(10), (13), and (17)–(20).

A new understanding on the breakdown of the Stokes-Einstein relation for colloidal suspensions was proposed on the basis that the distribution function of the velocities of the particles deviates from its equilibrium Gaussian form. Two mechanisms were in turn proposed to understand these deviations. At short times, during the intra-cage diffusion process, the velocities of the particles have not reached their equilibrium distribution due to confining forces [see Eqs. (6) and (9)], inducing a nonequilibrium energy transfer between the kinetic and the configurational degrees of freedom of the particles. The consequence is the appearance of an effective temperature larger than that of the heat bath [Eq. (10)] which modifies the Stokes-Einstein equation. This new result, together with our previously found expression for the viscosity of suspensions,[19] leads us to obtain an expression for the diffusion coefficient at short times, Eq. (2), that agrees extremely well with the experimental data.

The long-time breakdown is due to the fact that diffusion occurs as a sequence of thermally activated hopping processes between cages and, therefore, is characterized by rate and length coefficients that depend on the volume fraction. The rate coefficient is affected by the existence of attractive hydrodynamic interactions leading to the formation of temporary clusters. These structures are responsible for the dynamic arrest in the system and the breakdown of the Stokes-Einstein relation. The corresponding effective temperature is smaller than the bath's temperature and the comparison of our result for the diffusion coefficient, Eq. (18), with experimental data is very satisfactory.

Both approaches can be interpreted in a unified fashion if one considers that the thermally activated process, associated to the diffusion equation, Eq. (12), is related to an intermittent behavior of the velocities of the particles in such a way that, when the cages open and the particles jump from one cage to another, the distribution of velocities also deviates from its equilibrium Gaussian form.[30] In this case, an effective temperature smaller than that of the heat bath should appear that characterizes the breakdown of the Stokes-Einstein relation. This intermittent behavior is actually implicit in the thermally activated hopping process we used to calculate the long-time diffusion coefficient.

Finally, we used a DEMT to calculate interpolating functions for the effective diffusion and the viscosity of hard and porous spheres valid for both short and long times [see Eqs. (11) and (19)]. Although simple, these closed expressions are very accurate and fit experimental and numerical data remarkably well.

Summarizing, in this contribution, we have shown that the breakdown of the Stokes-Einstein relation at short and long times can be explained in terms of the deviation of the particles velocity distribution from their equilibrium Gaussian form, leading in turn to the appearance of effective temperatures. We also provided very accurate and simple formulas that provide a description which complements the procedures and views of hydrodynamic theories.

[1]G. C. Abade, B. Cichocki, M. L. Ekiel-Jeżewska, G. Nägele, and E. Wajnryb, J. Chem. Phys. **132**, 014503 (2010).

[2]G. C. Abade, B. Cichocki, M. L. Ekiel-Jeżewska, G. Nägele, and E. Wajnryb, J. Phys.: Condens. Matter **22**, 322101 (2010).

[3]G. C. Abade, B. Cichocki, M. L. Ekiel-Jeżewska, G. Nägele, and E. Wajnryb, J. Chem. Phys. **134**, 244903 (2011).

[4]D. Bonn and W. K. Kegel, J. Chem. Phys. **118**, 2005 (2003).

[5]W. van Megen, T. E. Mortensen, S. R. Williams, and J. Muller, Phys. Rev. E **58**, 6073 (1998).

[6]S. Jabbari-Farouji, D. Mizuno, M. Atakhorrami, F. C. MacKintosh, C. F. Schmidt, E. Eiser, G. H. Wegdam, and D. Bonn, Phys. Rev. Lett. **98**, 108302 (2007).

[7]F. H. Stillinger, Science **267**, 1935 (1995).

[8]C. A. Angell, Chem. Rev. **102**, 2627 (2002).

[9]G. D. J. Phillies, Macromolecules **17**, 2050 (1984).

[10]A. L. Kholodenko and J. F. Douglas, Phys. Rev. E **51**, 1081 (1995).

[11]N. Pottier, Phys. A **345**, 472 (2005).

[12]M. Tokuyama and I. Oppenheim, Phys. A **216**, 85 (1995).

[13]A. J. Banchio, G. Nägele, and J. Bergenholtz, J. Phys. Chem. **111**, 8721 (1999).

[14]P. N. Pusey and W. van Megen, Nature **320**, 340 (1986).

[15]R. H. Orttewill and N. St. J. Williams, Nature **325**, 232 (1987).

[16]A. van Veluwen and H. N. W. Lekkerkerker, Phys. Rev. A **38**, 3758 (1988).

[17]W. van Megen and S. M. Underwood, J. Chem. Phys. **91**, 552 (1989).

[18]E. R. Weeks, J. C. Crocker, A. C. Levitt, A. Schofield, and D. A. Weitz, Science **287**, 627 (2000).

[19]C. I. Mendoza and I. Santamaría-Holek, J. Chem. Phys. **130**, 044904 (2009).

[20]I. Santamaría-Holek and A. Pérez-Madrid, J. Phys. Chem. B **115**, 9439 (2011).

[21]B. J. Zwolinski, H. Eyring, and C. E. Reese, J. Phys. Chem. **53**, 1426 (1949).

[22]S. Glasstone, K. J. Laidler, and H. Eyring, *The Theory of Rate Processes* (McGraw-Hill, New York, 1941).

[23]I. Santamaría-Holek, J. M. Rubi, and A. Pérez-Madrid, New J. Phys. **7**, 35 (2005).

[24]D. Bedeaux, R. Kapral, and P. Mazur, Phys. A **88**, 88 (1977).

[25]C. W. J. Beenakker and P. Mazur, Phys. A **120**, 388 (1983).

[26]C. W. J. Beenakker and P. Mazur, Phys. A **131**, 311 (1985).

[27]P. Mazur and W. van Saarloos, Phys. A **115**, 21 (1982).

[28]Van P. Carey, *Statistical Thermodynamics and Microscale Thermophysics* (Cambridge University Press, Cambridge, 1999).

[29]C. I. Mendoza, J. Chem. Phys. **135**, 054904 (2011).

[30]M. Naspreda, D. Reguera, A. Pérez-Madrid, and J. M. Rubi, Phys. A **351**, 14 (2005).